Tribology International 92 (2015) 519–532

Contents lists available at ScienceDirect

Tribology International

journal homepage: www.elsevier.com/locate/triboint

A new approach for detection of wear mechanisms and determination of tool life in turning using acoustic emission

Luis Henrique Andrade Maia [a,*], Alexandre Mendes Abrao [b], Wander Luiz Vasconcelos [c], Wisley Falco Sales [d], Alisson Rocha Machado [d]

[a] UFMG/PUC Minas - Graduate Program in Mechanical Engineering Brazil
[b] UFMG - Graduate Program in Mechanical Engineering Brazil
[c] UFMG - Graduate Program in Metallurgical and Materials Engineering Brazil
[d] UFU - Graduate Program in Mechanical Engineering Brazil

ARTICLE INFO

Article history:
Received 24 March 2015
Received in revised form
15 July 2015
Accepted 21 July 2015
Available online 7 August 2015

Keywords:
Tool wear mechanisms
Acoustic emission
Power spectral density
Auto-covariance
Turning of hardened steel

ABSTRACT

A methodology for detection of wear mechanisms and determination of end of life of the cutting tool based on the acoustic emission signals is proposed, using an innovative technique. With this technique, the AE signals generated in hardened AISI 4340 steel turning respond well to the tool wear evolution. The tests were made using common and nanostructured AlCrN coated and uncoated cemented carbide tools. The AE signal spectrum is correlated with the wear mechanisms identified in the cutting tools and compared to the excitation frequency values corresponding to the respective mechanisms validating the identification of the wear mechanisms. The evolution of maximum flank wear resulted in increasing amplitude of average of Power Spectral Density at the end of life.

1. Introduction

Since the advent of polycrystalline cubic boron nitride (PcBN) tools, hard turning has been presented as an alternative to grinding. In hard turning, the workpiece is subjected to heat treatment prior to machining and the required roughness and tolerances are obtained without the need of abrasive operations. Bartarya and Choudhury [1] state that the success of hard turning depends on achieving certain requirements in relation to the machine tool, cutting tool and cooling conditions, among other factors, thus confining this operation to particular situations. Owing to the fact that hard turning involves more resistant work materials, machining forces are higher, therefore the use of tool materials with low coefficient of friction is essential. Polycrystalline cubic boron nitride (PcBN) and mixed alumina (Al_2O_3+TiC) are widely used for this application and, more recently, the development of coatings and micro-grained tungsten carbide tools has increased the range of materials capable of tackling hard turning.

Several authors [2–4] claim that PcBN is the first choice for hard turning, followed by aluminum oxide based ceramics due to the fact that these materials combine the required critical properties, such as high hardness and low chemical affinity with the work material. Camargo et al. [5] used PcBN cutting tools for turning of AISI D6 hardened steel (57 HRC) and produced a mathematical model based on multiple regression analysis to estimate tool wear. The dominant wear mechanisms were abrasion and attrition. Micro-chipping was also observed. With the generated model the cutting conditions could be estimated aimed at minimizing tool wear without compromising production rate. Sahoo [3] conducted turning tests with AISI 4340 steel (47 HRC) using cemented carbide tools without coating and with multilayer coatings (TiN, TiCN, Al_2O_3 and TiN) and (TiN, TiCN, Al_2O_3 and ZrCN) and observed that the coating has great influence on the tool performance. The best performance was provided by the (TiN, TiCN, Al_2O_3 and TiN) coated tool due to its lower coefficient of friction and stability at high temperatures.

The exact time of tool change is still a challenge for the metalworking industry and subject of continuous studies in the scientific community. Some of these studies take into account indirect techniques for continuous monitoring, this probably being the most appropriate way to address the matter. This type of monitoring is widely used in manufacturing processes due to the difficulty of monitoring the directly involved parameters. Acoustic emission (AE) is a possibility in the case of indirect monitoring. The use of acoustic emission is already quite widespread, especially for monitoring static equipment such as pressure vessels.

* Corresponding author.
E-mail addresses: luismaia@pucminas.br (L.H.A. Maia), abrao@demec.ufmg.br (A.M. Abrao), wlv@demet.ufmg.br (W.L. Vasconcelos), wisley@ufu.br (W.F. Sales), alissonm@mecanica.ufu.br (A.R. Machado).

http://dx.doi.org/10.1016/j.triboint.2015.07.024
0301-679X/

The energy released by a body when it is altered/removed from its original state/form emits sound. Thus, corrosion, forming, wear, shear, tensile and compression mechanisms are generators of acoustic emission in a body. The application of this technique in machining is still hampered by several mechanisms and phenomena in cutting which are still not completely understood. The frequencies at which some phenomena such as movement of dislocations, voids coalescence, twinned training, etc. happen are not well known. Furthermore, the contribution of temperature and wear and frictional processes in the workpiece-tool pair further complicates the system. In spite of that, AE is a promising technique for monitoring cutting tool wear and has been widely used in grinding [6,7] as well as in the machining with geometrically defined tools. Hase et al. [8] monitored the AE signals when turning a mold steel (AISI O1) with cermet tools and correlated the signals with the cutting phenomena. They noticed that the chip formation process, the chip form and the primary shear angle affected significantly the AE signals. The correlation with the workpiece surface finish and tool wear was also determined.

According to Li [9], acoustic emission is a wave of tension that travels through the material as a result of some sudden release of tensile energy. It can also be defined as the elastic energy released spontaneously during a local, dynamic and irreversible change in the microstructure of the material. Several natural phenomena such as earthquakes, avalanches, landslides and crack propagation in ice are accompanied by acoustic emission [10]. The peculiarity of the acoustic emission signal involved in tribological processes is the necessity to understand how the elastic interaction of surface roughness is converted into acoustic emission signals [11]. Hase et al. [12] studied the characteristics of the acoustic emission signals and correlated them with the wear mechanisms. They determined the frequency bands and voltage amplitude of the AE signals from several studies involving the phenomena and highlighted that abrasive wear covers a wide frequency band (from 250 kHz to 1 MHz), but the peaks are well characterized and can serve as a basis to identify which mechanism prevails in the experiment. Crack propagation acts in the range of 100 kHz to 700 kHz and therefore overlaps the excitement generated by abrasive wear. Adhesion and movements on the surface (stick-slip phenomenon) excites a narrow band (25–110 kHz) and overlap adhesive wear and particle interactions. Adhesive wear is classified into mild and severe wear, each of them exciting a different frequency band. In mild adhesive wear, rolling and collision of particles on the wear surface excites the frequency band of 10–100 kHz, while in severe wear transfer of particles between the surfaces excites from 1 to 1.5 MHz [13]. Hase et al. [12] confirm this statement and highlight that adhesive wear occurs with peaks in the frequency of 1.1 MHz. The other mechanisms have very characteristic peaks and promote a much narrower excitation band than abrasive wear.

Due to the dynamic cutting action occurring in machining, the tool wears out while the shape of the chip and the phase of the material can change, thus causing a variation in the AE spectrum. A compilation from various studies is presented in Table 1, which summarizes the principal mechanisms and the respective excited frequencies of the AE signal.

Ferrer et al. [18] studied the effects of stick and slip between two metal surfaces and analyzed the acoustic emission signals produced by this phenomenon. The authors changed the compressive force, the relative displacement speed between the bodies and the contact surface geometry. The AE signals produced by this phenomenon excited a frequency range from 25 kHz to 110 kHz with a peak of 105 kHz.

The sources of acoustic emission signals in metals can be divided basically into three [20]: the first one is related to mechanisms that induce plastic deformation and to atomic movement processes (annihilation of dislocations and generation of dislocations by the Frank-Read mechanism), twinning and grain boundary sliding. The second source refers to mechanisms associated with first and second order phase transformations: polymorphic transformations including martensitic transformation, the second phase particle formation in supersaturated solid solution decomposition, phase transition magnetics and superconductors, magnetic and mechanical phenomena due to the contour changes and reorientation of a magnetic field with a variation of the external magnetic field. Finally, the third source takes into account mechanisms for damage such as origin and micro-defects accumulation, nucleation and growth of cracks and corrosive damage including corrosive cracking.

Table 1
AE signals frequencies of principal exciter phenomena in ordinary materials.

Phenomenon	AE frequency range (kHz)
Machining [14]	70–115
White layer [15]	>60
Isothermal phase transformation [16]	250–350
Mild adhesive wear [17]	0–120
Severe adhesive wear [17]	1000–1500
Adhesion and dragging [18]	25–110
Movement of dislocations [13]	10–220
Particle interaction [19]	120–350
Abrasive wear [8,13]	200–1000
Crack propagation [20,21]	350–550
Phase transformation [16]	350–550
Accommodation of vacancies [22]	220–380
Annihilation of dislocations [20]	100
Frank-Read dislocation [20]	1000
Plastic deformation [20]	50
Plastic deformation [20,17]	150–500
Elastic deformation [13]	25–250
Thermal noise [20]	10–100

Chung et al. [19] studied particles interaction in hard disks when subjected to SiC and polystyrene injection mechanisms and subsequent wear on their surface. A particle injection system in which the hard disk run and maintained contact with a mechanism responsible for spreading SiC and polystyrene particles (with a diameter of 0.9 mm) on its surface was used. The signals from contact between the hard (SiC) and soft particles (polystyrene) and their deposition on the surface excited a frequency from 200 kHz to 350 kHz.

Mostafapour et al. [16] applied the wavelet technique and the time and frequency crossed spectrum to determine the acoustic emission source with varying frequency and speed of wave on a plate with an arrangement consisting of four AE sensors. The graphite breaking technique was applied on the plate at random points for the generation of acoustic emission signals, which were decomposed by wavelet in the range from 125 kHz to 250 kHz, then generating the crossed spectra of time and frequency. The signals are crossed and the delay time is calculated when the spectrum reaches its maximum amplitude while the wave velocity is calculated using the maximum frequency, which is captured from this maximum value. The wave speed determines the time delay between the sensors showing the position of the event. The authors concluded that the application of this technique is more accurate than the current correlation method in most software used for AE signals monitoring.

Marinescu and Axinte [14] studied the effectiveness of acoustic emission signals in the detection of failure in double-coated (TiAlN+TiN) carbide tools in milling operation of Inconel 718. The authors compared the AE signals with the signals of the cutting forces and demonstrated that AE has a greater sensitivity to wear.

This work proposes to monitor the acoustic emission signal (AE) and to correlate it to tool wear and wear mechanisms using an innovative methodology, i.e., Power Spectral Density—PSD and auto-covariance, when turning hardened AISI 4340 steel. The excitation frequency of the AE signals was correlated with the principal wear mechanisms identified by scanning electron microscopy (SEM) analysis and compared with the AE signal excitation frequencies available in literature (Table 1) for validation of the method.

2. Experimental procedure

Bars of AISI 4340 steel with a hardness of 46 ± 1 HRC were used as work material. ISCAR uncoated cemented carbide inserts ISO grade K10-20 with geometry ISO SNMA 120408 (without chip breaker) were used as cutting tools. The inserts were mounted on an ISCAR ISO DSBNR 2525M12 coded toolholder. Although this grade is indicated for machining of cast iron, it was selected due to the absence of chip breaker (flat rake face), not available for steel cutting tungsten carbide grades. Part of the inserts was coated at Oerlikon Balzers (Brazil). One half of them received a monolayer of AlCrN and the other half received a monolayer of nanostructured AlCrN, both with a thickness 3 μm applied by physical vapor deposition (PVD). Another part of the inserts remained without coating and was used as control. Table 2 summarizes the characteristics of the inserts.

Turning tests were carried out on CNC lathe (power of 7.5 kW and maximum rotational speed of 4000 rpm). For the acquisition of the acoustic emission signals, a Physical Acoustics R15i piezoelectric transducer (frequency response curve shown in Fig. 1) connected to a Spartan 2000 signal conditioner were used. The conditioned signals were acquired using a PCI-6251 board manufactured by National Instruments (maximum acquisition rate of 1.2 Mb/s) installed in an AMD Fusion A8 computer (Quad-Core 2.9 GHz with 4 MB cache) with video card Radeon Vision HD6550D, RAM memory DDR3 1333 of 8 GB and hard disk of 1TB. Tool wear was measured using a Mitutoyo TM15 optical stereomicroscope with magnification of 15× and micrometer head with resolution of 1μm.

Turning trials were performed dry using two cutting conditions as follows: (a) cutting speed (v_c) of 200 m/min, feed rate (f) of 0.15 mm/rev and depth of cut (a_p) of 0.25 mm and (b) cutting speed (v_c) of 250 m/min, feed rate (f) of 0.20 mm/rev and depth of cut (a_p) of 0.25 mm. These parameters were selected following recommendations from the tool manufacturer as they are typically used for cemented carbide tools. The AE signals were collected for 2 s during the turning tests at the beginning and the middle of each pass. The acoustic emission signals were collected using the piezoelectric sensor fixed on the tool holder and acquired using software specifically designed for this purpose in the Labview platform. The acquisition was carried out at a rate of 1200 kHz (due to continuous acquisition, which generates a large amount of data) and the Nyquist theorem states that the data collected at this rate allows the analysis of frequencies up to 600 kHz. In addition to that, a high pass active FIR (Finite Impulse Response) filter of 10 kHz was used. According to Williams and Taylor [23], the advantages of the FIR filter resides in the fact that it can be designed with linear phase and performed as recursive or non-recursive. Moreover, it allows any filtration function by scaling the coefficients, which makes it largely stable, becoming ideal for adaptive signal processing. As the AE signals are extremely sensitive to various excitations, including the mechanisms of deformation and movement and generation of defects, tensile tests were conducted on the work material and the acoustic emission signals generated by deformation were identified for further separation from the signals generated by tool wear mechanisms when machining.

Table 2
Characteristics of the cutting tools used in the experimental work.

Code	ISO grade	ISO geometry	Coating
A	K10–20	SNMA120408	Without coating
B	K10–20	SNMA120408	PVD (AlCrN)
C	K10–20	SNMA120408	PVD (AlCrN nanostructured)

Fig. 2 shows the steps for processing the acoustic emission signals. The signals from the turning tests were initially subjected to a "cut range" FIR active filter of 144–156 kHz, which is the excitation range of deformation of hardened AISI 4340 steel. The resulting signals were subjected to the amplitude modulation technique applied with a carrier wave frequency of 200 kHz. This modulated signal was squared (B) and summed to the square of the filtered signal (A) and then the square root was extracted. This result was then submitted to auto-covariance analysis to remove the contribution of transient signals and then analyzed by the power spectral density (PSD) technique. The PSD technique provides the average frequency spectrum of the acquired signals, making possible the determination of the actual contribution of the tool wear mechanisms. Finally, the average PSD, which is the area of the PSD signal curve that gives the energy of the signal, was obtained. This energy was used to quantify the AE signal and to correlate it with the maximum flank wear (VB_{BMAX}).

Images of the tools were produced using a JEOL JSM—6306LV scanning electron microscope with analytical capacity for energy dispersive spectroscopy (EDS) in order to characterize the coatings. Before tool wear analysis, the inserts were etched in a

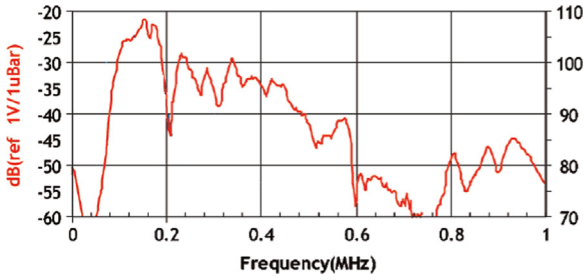

Fig. 1. Frequency response of the AE sensor.

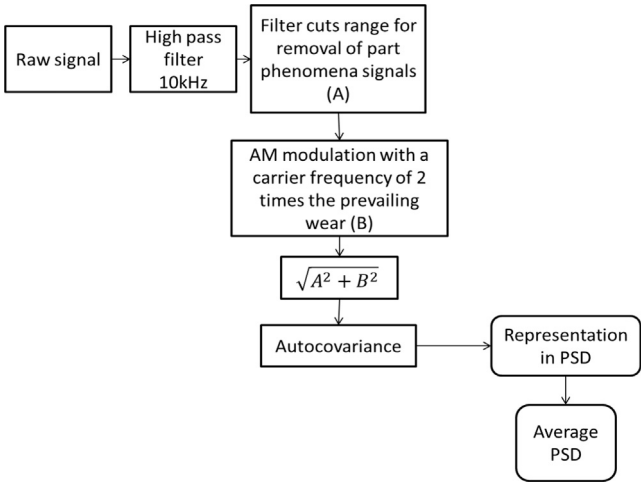

Fig. 2. Processing of acoustic emission signals.

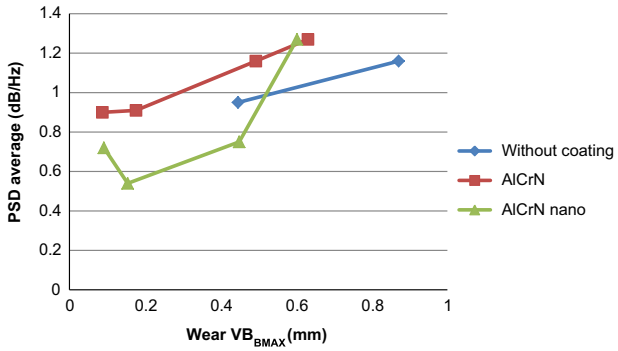

Fig. 3. PSD power in function of maximum flank wear in turning with cutting speed of 200 m/min, feed rate of 0.20 mm/rev and depth of cut of 0.25 mm.

solution of 30% of hydrochloric acid diluted in for 12 h in order to remove adhered work material.

3. Results and discussion

The PSD technique can be defined as the estimation of the distribution of the total power of the signal in the frequency domain from a finite recording of a sequence of stationary data [24]. In summary, the signals generated by the PSD technique behave as follows: random signals (no repetitions) generate lines without inclination, while periodic signals generate spikes with recurring frequency characteristic of the signal. The amplitude modulation aims to strengthen the amplitudes of the excited frequencies in the frequency band of the modulator, thereby increasing the sensitivity to excitation variations. Combining amplitude modulation with the auto-covariance technique (effective in eliminating noise), it is possible to differentiate the beginning of life from the end of life signals, which is not possible with such accuracy using other methods.

Fig. 3 shows the influence of tool wear on the average PSD when turning at cutting speed 200 m/min, feed rate 0.20 mm/rev and depth of cut 0.25 mm. Maximum flank wear (VB_{BMAX}) of 0.44 mm with an average PSD of 0.95 dB/Hz was recorded for the uncoated tool. In the second pass, the average PSD reached a value of 1.16 dB/Hz with $VB_{BMAX}=0.87$ mm. The average PSD value followed the trend observed in other tests where the AE signal strength at the beginning of life is smaller than at the end of life. For the AlCrN coated tool, the average PSD was 0.9 dB/Hz in the first pass ($VB_{BMAX}=0.087$ mm) and increased to 0.91 dB/Hz in the second pass ($VB_{BMAX}=0.176$ mm). In the third and fourth passes, the inclination of the curve remained constant, which indicates a good linear correlation between the average PSD and maximum flank wear. For the nanostructured AlCrN coated tool, maximum flank wear of 0.091 mm was observed in the first pass, when the average PSD was 0.72 dB/Hz, suffering attenuation in the second pass and to 0.54 dB/Hz with $VB_{BMAX}=0.154$ mm. In the third pass, the average PSD increased again reaching 0.75 dB/Hz with a $VB_{BMAX}=0.449$ mm and in the last pass the average PSD reached 1.27 dB/Hz for $VB_{BMAX}=0.602$ mm.

The waveforms and frequencies spectra of the AE signals when turning at cutting speed 200 m/min, feed rate 0.20 mm/rev and depth of cut 0.25 mm are shown in Fig. 4. For the high acquisition rate (1.2 MHz), the waveforms (Fig. 4a, c and e) did not show variations that can be used to evaluate the wear mechanisms of the tools. The spectra of the tools (Fig. 4b, d and f) suggest slight differences among the tools, particularly between the coated AlCrN tool and the others. The spectrum analysis is a resourceful method and widely used by several authors [25–27], however, the sensitivity of this can lead to an erroneous assessment. The use of PSD coupled to auto-covariance suppresses this drawback by generating signals free of noise and sensitive only to tool wear mechanisms. The employed technique allows the elimination of noise and the magnification the signals associated with wear mechanisms through the signal sum enveloped with the raw signal, thus demonstrating tool wear evolution detecting the end of tool life.

Maximum flank wear evolution with cutting time when turning at cutting speed of 200 m/min, feed rate of 0.20 mm/rev and depth of cut of 0.25 mm is presented in Fig. 5, where it can be noted that the lifetime of the uncoated tool is shorter than that of the coated tools AlCrN ((212 s against 424 s for both coated tools). This behavior can be explained by the barrier imposed by the coatings, which inhibits wear mechanisms. Table 3 shows selected properties and characteristics of coatings which lead to improved performance before wear conditions.

The PSD values when turning with the uncoated tool at cutting speed 200 m/min, feed rate of 0.20 mm/rev and depth cut of 0.25 mm is shown in Fig. 6, where it can be seen that the frequency range between 0 and 90 kHz is excited at the beginning of the cut, thus indicating adhesive wear. Wada and Mizuno [17] studied adhesive wear mechanisms using pin on disk tests with acoustic emission sensors and noticed that adhesive wear excites a wide frequency range (from 0.01 to 1.5 MHz). Mild wear is characterized by rolling and collision of particles at the wear surface, which excites the range 10–100 kHz. On the other hand, severe adhesive wear is excited by particulate transfer between surfaces and excites from 1 to 1.5 MHz.

The frequency range between 200 kHz and 500 kHz is related to both crack propagation and abrasive wear. It is excited at the beginning of cut with low PSD energy, suggesting that there is little impact of tool wear at the beginning of cut. Hase et al. [28] claim that abrasive wear mechanism excites the 200–1000 kHz band. The authors emphasize that in abrasive wear, the sliding surface is grooved by abrasive grains. In this case cutting (shear fracture) and the formation of grooves (plastic deformation) occur between the abrasive grain contact area with the sliding material generating the characteristic wear surface. The energy released by plastic deformation is lower than that released by the fracture and this makes the fracture to be the main source of AE in abrasive wear, exciting the band between 200 kHz and 500 kHz. Wada et al. [13] showed that the signal amplitude is determined by the size of the abrasive grain and that the band near 500 kHz is excited by abrasive wear. The band between 250 Hz and 1000 Hz is due to the variation of excitation mechanisms in abrasive wear, characterized by shearing and plowing of the surface [12]. Baranov [20] states that crack propagation excites the band near 500 kHz. Ramadan et al. [21] monitored corrosion and the formation of microcracks and showed that the band between 100 and 300 kHz is excited by microcrack formation. The analysis of the SEM micrograph of the cutting edge after the first pass (Fig. 7a) does not suggest the presence of microcracks, nevertheless it indicates the occurrence of microabrasive wear. The PSD signal at end of tool life shows that the frequency band 0–90 kHz is still excited (adhesive wear) and that the band between 200 kHz and 550 kHz is also excited with low energy.

Diffusive wear is the most dominant mechanism in the uncoated tool at cutting speed of 200 m/min, feed rate 0.20 mm/rev, and cutting depth 0.25 mm. The smooth aspect of the tool surface indicates diffusive wear, as demonstrated by Trent and Wright [29]. Furthermore, the cobalt used as a binder in cemented carbide has great affinity with iron and promotes this mechanism [30]. According to Holmberg and Matthew [31], diffusion wear characterizes the material loss due to diffusion of atoms of the tool material into the workpiece moving over it. Requirements for diffusion wear are metallurgical bonding of the two surfaces so

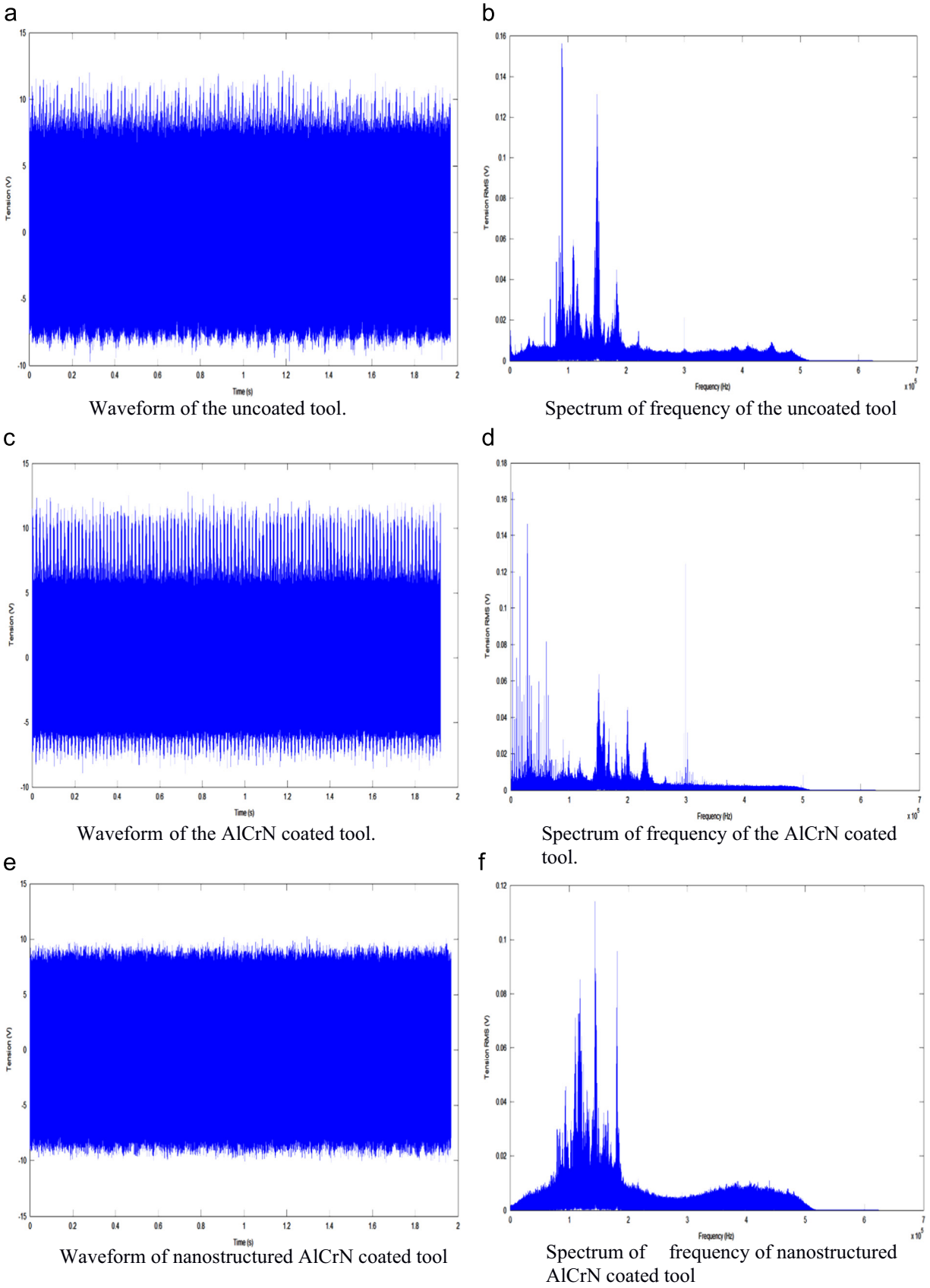

Fig. 4. AE signals when turning with cutting speed of 200 m/min, feed rate of 0.20 mm/rev and depth of cut of 0.25 mm using fresh tools. (a) Waveform of the uncoated tool. (b) Spectrum of frequency of the uncoated tool. (c) Waveform of the AlCrN coated tool. (d) Spectrum of frequency of the AlCrN coated tool. (e) Waveform of nanostructured AlCrN coated tool, (f) Spectrum of frequency of nanostructured AlCrN coated tool.

that atoms can move freely across the interface, temperature high enough to make rapid diffusion possible and some solubility of the tool material phases in the work material. Temperature and the flow rate in the region immediately adjacent to the surface are two major parameters influencing diffusion wear. Trent and Wright [25] state that diffusion wear is a sort of chemical attack on the tool surface (such as etching) and is dependent on the solubility of the different phases of the tool material in the metal flowing over the surface, rather than on the hardness of these phases. The carbide particles are more resistant because of their lower solubility in the work material. The rate of diffusion wear is very dependent on the metallurgical relationship between tool and work material and this is a critical aspect when cutting metals such as titanium or copper alloys.

Dolinsek and Kopac [32] assert that frequencies below 50 kHz are excited discontinuously and do not characterize the evolution of wear. Although this information is valid, the recent advances in signal acquisition methodologies have enabled spectrum-temporal analysis. Turning is a highly dynamic event and involves a number of phenomena which act alone or together. Similarly, the AE signals are susceptible to variations and compositions of events, which are sources of excitation, thus producing a discrete signal. Thus, the signals analyzed by PSD are a rich source of information and the discrete signals that are excited should not be ignored, especially with high energy such as the frequency of 32.81 kHz. This frequency suggests the presence of adhesion and dragging on the surface due to the relative movement between tool and workpiece, but it can also be related to the movement of dislocations on the tool, as indicated in Table 1.

After the first pass (Fig. 7a), diffusion wear characterized by a smooth surface is observed on the uncoated tool, in addition to a small amount of abrasive wear on the flank surface, which increases as the end of life is approached (Fig. 7b). Moreover, crater wear is observed on the rake face, see Fig. 7b, probably caused by adhesion and abrasion.

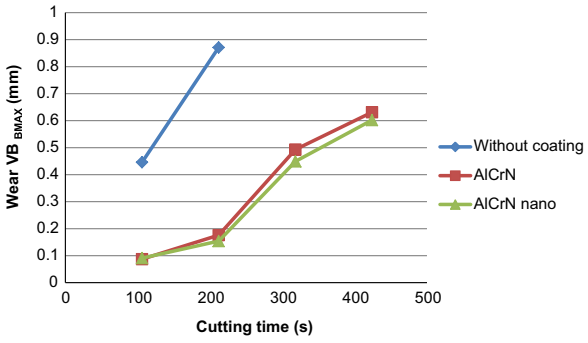

Fig. 5. Maximum flank wear against cutting time when turning with cutting speed of 200 m/min, feed rate of 0.20 mm/rev and depth of cut of 0.25 mm.

After turning, all tools presented work material adhered to the flank and rake faces, as can be seen in Fig. 8. Fig. 8a shows work material adhered to the rake face of the uncoated tool after two passes, while Fig. 8b shows the flank face of the AlCrN coated tool after four passes with a large amount quantity of adhered material. The same situation is observed in Fig. 8c, which shows the flank face of the nanostructured AlCrN coated tool with workpiece material adhered after 4 passes. According to the PSD signals, the most active mechanism is adhesive wear (higher amplitude excitation in the 0–90 kHz frequency band), which is confirmed by micrographs of tools before the removal of the adhered layer.

The PSD values recorded for the AlCrN coated tool when turning with cutting speed of 200 m/min, feed rate of 0.20 mm/rev and depth of cut of 0.25 mm (Fig. 9) show that the signals at the beginning and end of life present the same pattern, with a slight increase in amplitude at the end of tool life. The signals are excited in the frequency range from 0 kHz to 90 kHz, which is inherent of adhesive wear, and in the band from 250 kHz to 500 kHz, which is related to abrasive wear and crack propagation.

After the first pass of the AlCrN coated tool (Fig. 10a), typical abrasive wear grooves can be observed in the flank face, whereas the rake face shows the smooth aspect of diffusive wear. The maintenance of the AlCrN film allows the occurrence abrasive wear, however, diffusion wear is promoted after removal of the film due to the chemical affinity between iron (from the workpiece) and cobalt (from the tool). After the second pass (Fig. 10b) more and longer grooves can be found on the flank face, but the coating is maintained. At the rake face, more substrate material is removed, increasing crater wear. The third pass (Fig. 10c) leads to the removal of the coating on the flank face and then the diffusive mechanism appears together with abrasive wear. The last pass (Fig. 10d) shows the predominance of diffusive wear on the flank face, with abrasive wear concentrated at the interface. Adhered material was observed after all passes and the formation of microcracks was noted in none.

The PSD values for the nanostructured AlCrN coated tool when turning with a cutting speed of 200 m/min, feed rate of 0.20 mm/rev and depth of cut of 0.25 mm (see Fig. 11) show the same characteristics of the AlCrN coated tool (Fig. 9), with excitation of adhesive wear (0–90 kHz) and abrasive wear (200 kHz to 550 kHz) mechanisms and PSD values of lower amplitude at the beginning of tool life.

Fig. 12 shows SEM micrographs of the nanostructured AlCrN coated tool after turning with a cutting speed of 200 m/min, feed rate of 0.20 mm/rev and depth of cut of 0.25 mm. After the first pass (Fig. 12a), only abrasive wear is confirmed by the presence of grooves on the flank face. The coating is not removed from the rake face, where only abrasive wear is noted. After the second pass (Fig. 12b), the flank face presents abrasive wear with the removal of the coating (clearer area), which allows diffusion wear to take place, whereas the removal of the coating and the development of crater wear with evidence of diffusion can be seen on the rake

Table 3
Selected properties of the principal PVD coatings.

	TiN	TiCN	TiC	TiAlN	CrN	AlCrN	Al_2O_3
Coating process	PVD/CVD	PVD/CVD	PVD	PVD	PVD	PVD	CVD/PVD
Coating thickness (μm)	1–5	1–5	1–5	1–5	1–10	1–5	1–5
Microhardness (HV 0.05)	2300	3000	3100	3000	1900	3200	2100 HV 0.1
Oxidation temperature (°C)	> 450	> 350	> 350	> 700	> 600	> 800	–
Thermal effect barrier	+++	++	+	++++	+	++	+++++
Abrasion resistance	++	+++	+++	+++	++	++++	++
Adhesion wear resistance (against steel)	++	++	+	++	++	++	+++
Diffusion wear resistance (against steel)	++	+	+	+++	++	+++	+++
Protection of the substrate against corrosion	+	+	+	+	++	++++	+

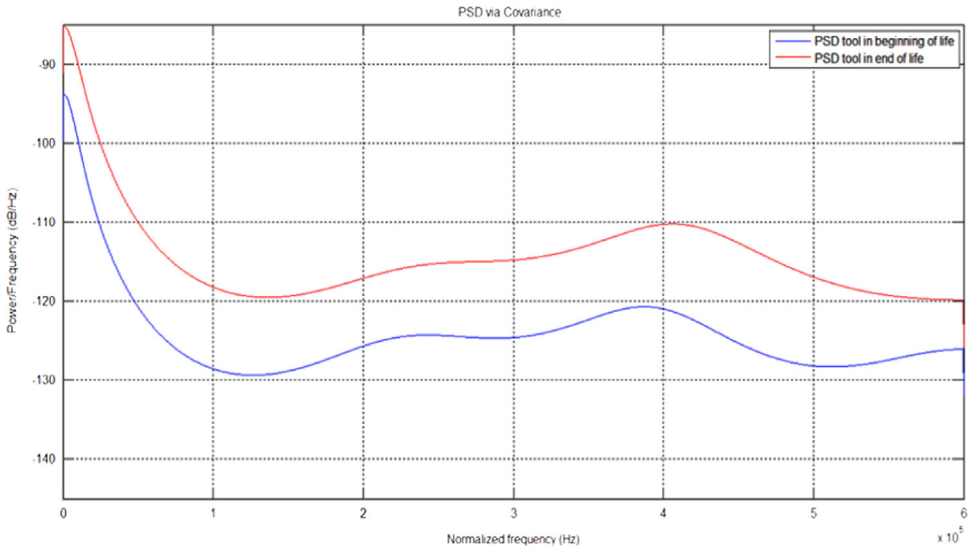

Fig. 6. PSDs of AE signals at the beginning and end of life of the uncoated tool when turning AISI 4340 steel with cutting speed of 200 m/min, feed rate of 0.20 mm/rev and depth of cut of 0.25 mm.

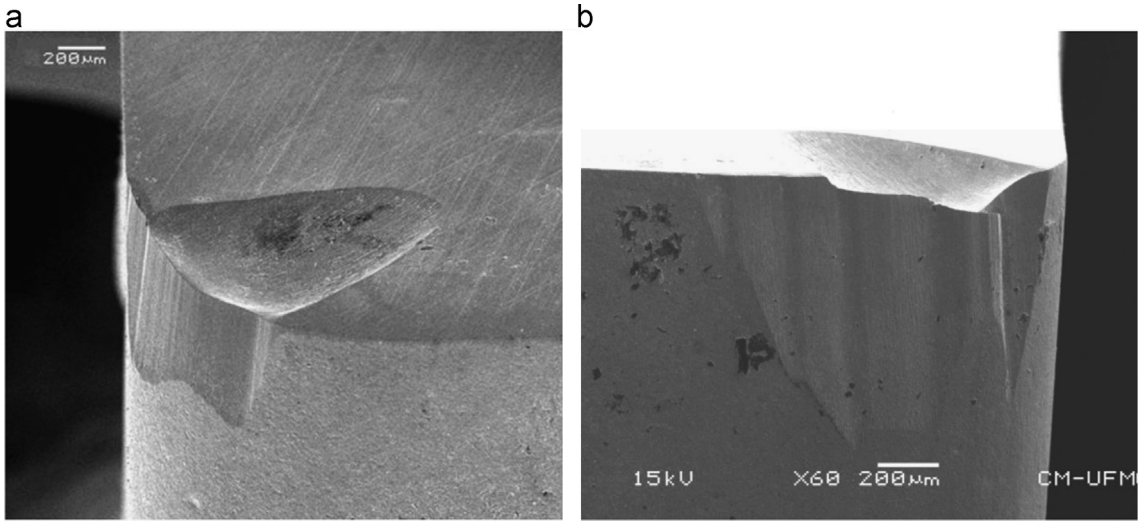

Fig. 7. SEM micrographs of a worn uncoated tool after turning with cutting speed of 200 m/min, feed rate of 0.20 mm/rev and depth of cut of 0.25 mm. (a) First pass, (b) second pass.

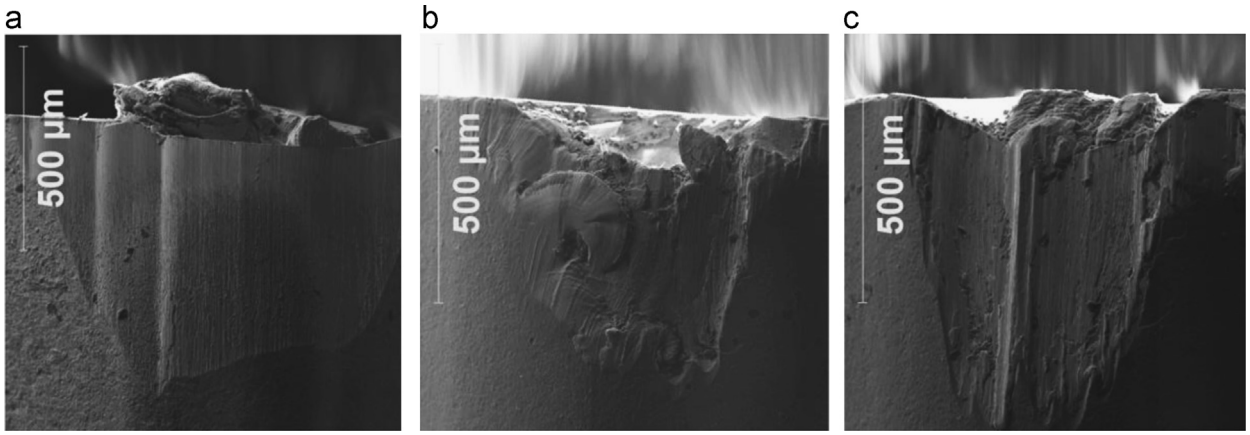

Fig. 8. SEM micrographs of worn tools after turning AISI 4340 steel with cutting speed of 200 m/min, feed rate of 0.20 mm/rev and depth of cut of 0.25 mm. (a) Without coating, (b) AlCrN, (c) nanostructure AlCrN.

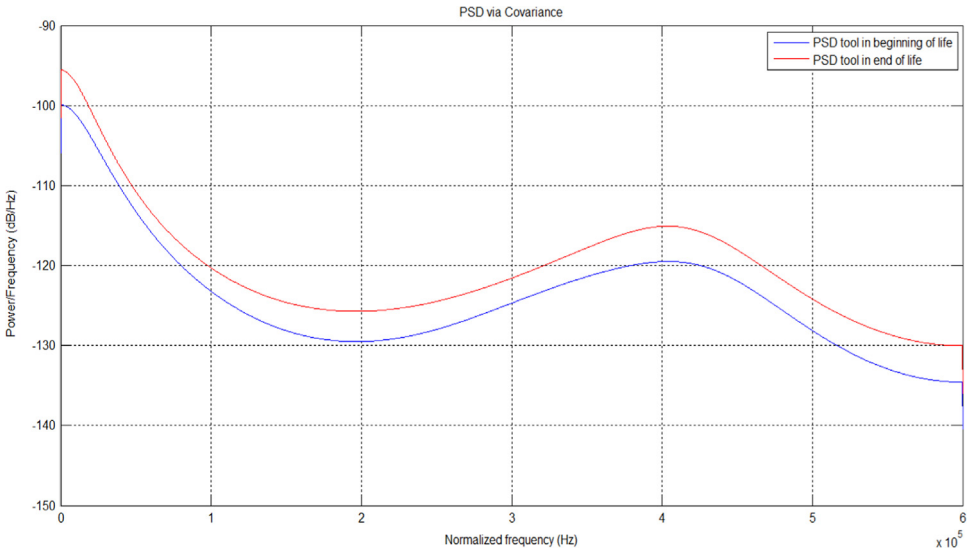

Fig. 9. PSDs of AE signals at the beginning and end of life of the AlCrN coated tool when turning AISI 4340 steel with cutting speed of 200 m/min, feed rate of 0.20 mm/rev and depth of 0.25 mm.

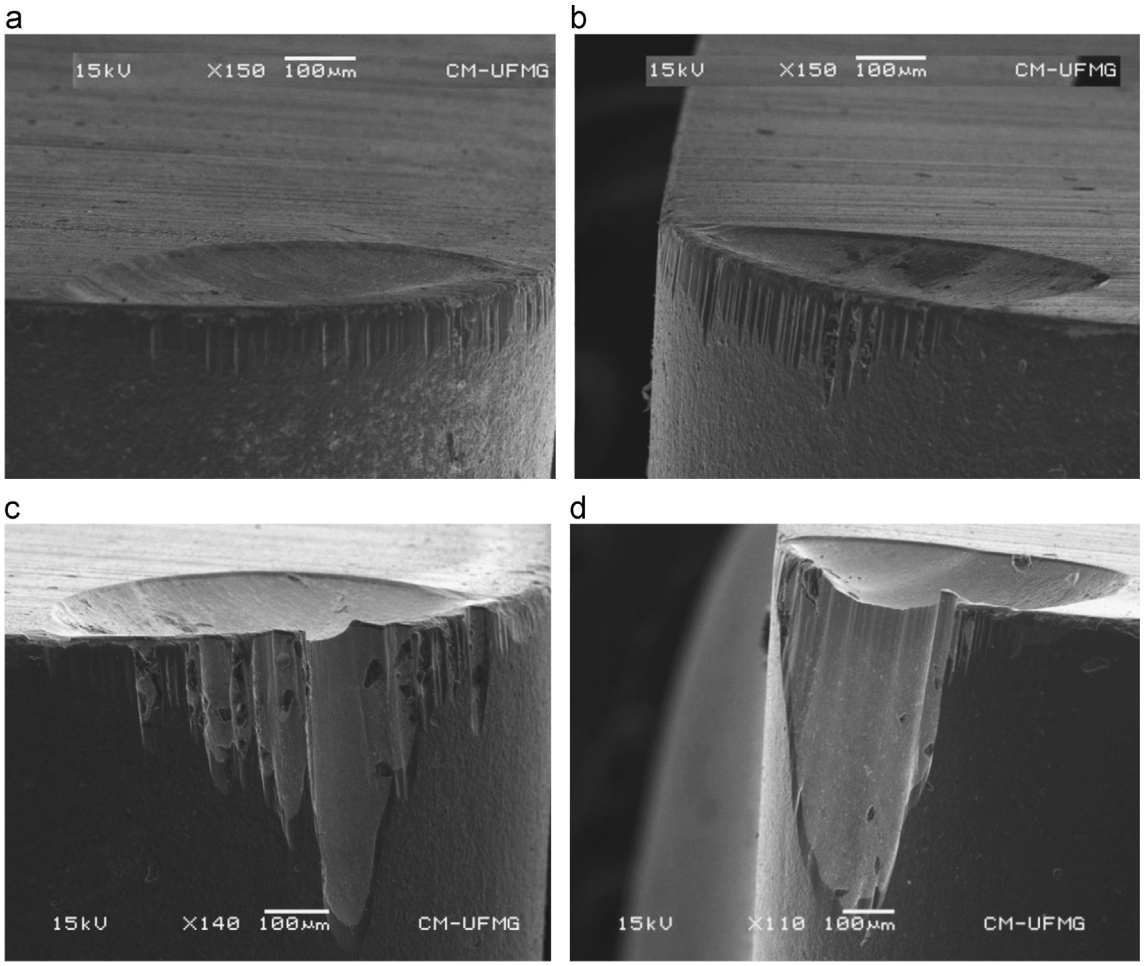

Fig. 10. SEM micrographs of a worn coated carbide tool after turning with cutting speed of 200 m/min, feed rate of 0.20 mm/rev and depth of cut of 0.25 mm. (a) First pass, (b) second pass, (a) First pass, (b)_Second pass, (c) Third pass and (d) Fourth pass.

face. Removal of the nanostructured AlCrN coating from the flank face can be observed after the third pass (Fig. 12c). Tool material is removed at high rate by diffusion wear, while abrasive wear is concentrated on the rake face and in the region where the coating was not removed. After the fourth pass (Fig. 12d), the flank face shows a smooth aspect typical of diffusive wear. Moreover, the large grooves indicate that even at low rate, abrasive wear still remains present as a wear mechanism. Diffusive wear increases the depth of the crater on the rake face and deteriorates the cutting edge.

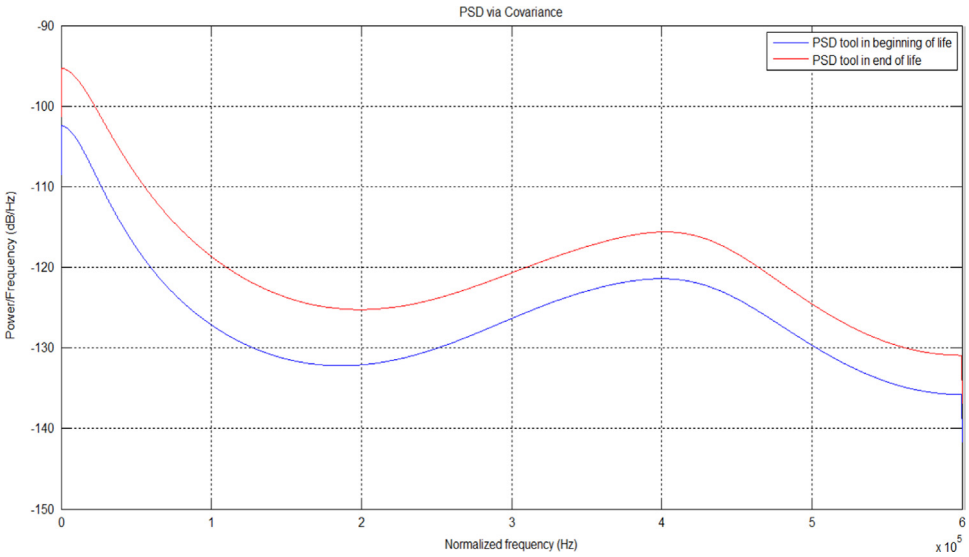

Fig. 11. PSDs of AE signals at the beginning and end of life of the nanostructured AlCrN coated tool when turning AISI 4340 steel with cutting speed of 200 m/min, feed rate of 0.20 mm/rev and depth of cut of 0.25 mm.

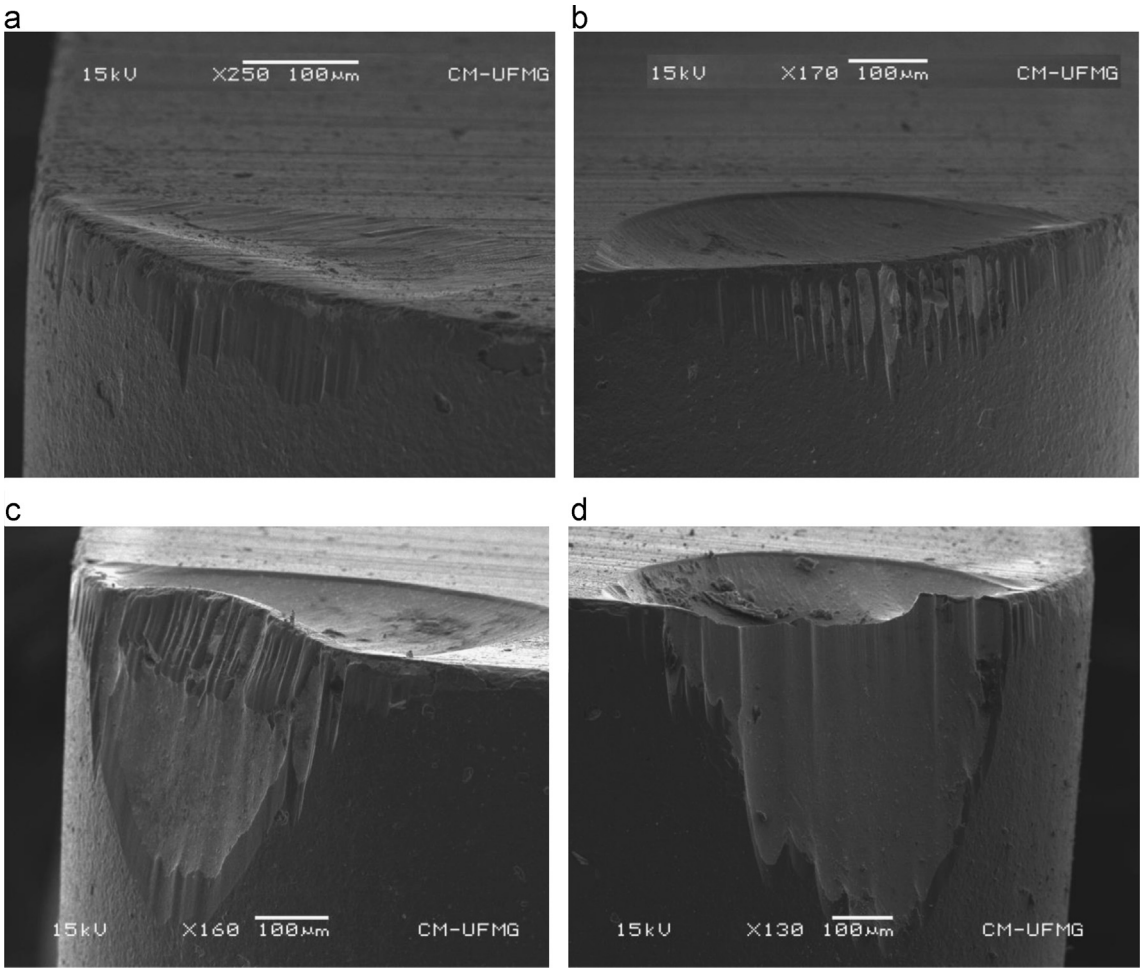

Fig. 12. SEM micrographs of a worn nanostructured AlCrN coated tool after turning with cutting speed of 200 m/min, feed rate of 0.20 mm/rev and depth of cut of 0.25 mm. (a) First pass, (b) second pass, (c) third pass, (d) fourth pass.

The relationship between the average PSD value and maximum flank wear when turning with cutting speed of 250 m/min, feed rate of 0.15 mm/rev and depth of cut of 0.25 mm is shown in Fig. 13. After the first pass the uncoated tool presented $VB_{BMAX}=0.544$ mm with an average PSD of 0.46 dB/Hz. In the second pass, the average PSD reached a level of 1.05 dB/Hz with $VB_{BMAX}=1.372$ mm, following the trend of a lower signal strength at the beginning of life compared to the end of life. For the AlCrN coated tool, in the first pass the average PSD was 0.94 dB/Hz with $VB_{BMAX}=0.245$ mm. The average PSD was reduced to 0.26 dB/Hz

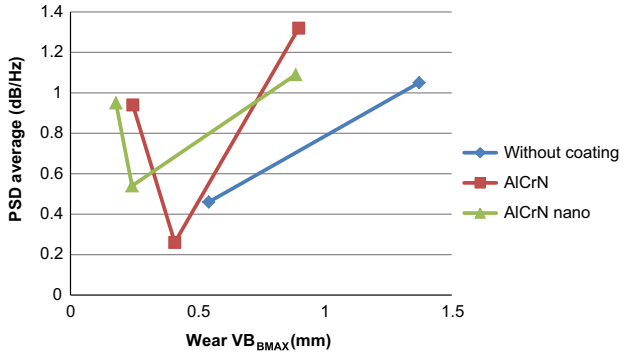

Fig. 13. PSD power against maximum flank wear when turning with cutting speed of 250 m/min, feed rate of 0.15 mm/rev and depth of cut of 0.25 mm.

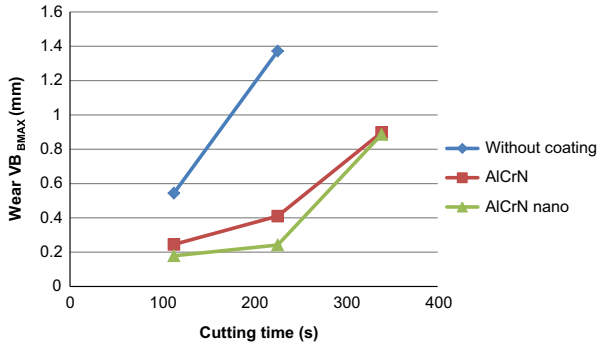

Fig. 14. Maximum flank wear against cutting time when turning with cutting speed of 250 m/min, feed rate of 0.15 mm/rev and depth of cut of 0.25 mm.

after the second pass with $VB_{BMAX}=0.41$ mm and during the third pass the average PSD increased to reach 1.32 dB/Hz with $VB_{BMAX}=0.898$ mm. The larger PSD value found in the first pass and its subsequent reduction in the second pass can be explained by the decrease in the tool wear rate observed under intermediate and high material removal rates. The maximum flank wear of the nanostructured AlCrN coated tool after the first pass was $VB_{BMAX}=0.179$ mm with an average PSD of 0.95 dB/Hz. During the second pass the average PSD was reduced to 0.54 dB/Hz with a corresponding maximum flank wear of 0.242 mm. In the third pass the average PSD increased to 1.09 dB/Hz with $VB_{BMAX}=0.886$ mm, following the trend of the AlCrN coated tool. The AlCrN coated tool presented higher flank wear rate compared to the nanostructured AlCrN coated tool, thus resulting in larger variation in the average PSD values. Considering that the cutting edge is subjected to scratching conditions, the material will undergo a series of phenomena. Elastic and plastic deformations followed by fracture excite several different frequencies [33]. These events associated with the decrease in hardness of the cemented carbide under high temperature lead to the instantaneous variation of the excited frequencies, especially for the uncoated and AlCrN coated carbide tools due to the fact that a variation in the tool-workpiece interface caused by a change in the hardness of the tool affects the wear mechanisms and, consequently, the AE signals.

The effect of cutting time on the maximum flank wear when turning with cutting speed of 250 m/min, feed rate of 0.15 mm/rev and cutting depth of 0.25 mm is shown in Fig. 14, where it can be noted that the coated tools outperformed the uncoated insert by approximately 50%. In addition to that, the lower flank wear rates recorded for the coated tools confirm the ability of the film to act as an effective barrier against the wear mechanisms present in metal cutting.

Fig. 15 shows the presence two peaks in the average PSD at the beginning of life and end of tool life when turning using the uncoated tool with cutting speed of 250 m/min, feed rate of 0.15 mm/rev and depth of cut of 0.25 mm. The first peak is characteristic of adhesive wear (frequency range from 0 to 90 kHz) and the second refers to abrasive wear (from 300 kHz to 525 kHz). Evidence of microcracks was not found, as can be seen in Fig. 16. Furthermore, the uncoated tool showed the same characteristics after the first and second passes (Fig. 16a and b, respectively) when turning at a cutting speed of 250 m/min, feed rate of 0.15 mm/rev, and depth of cut of 0.25 mm, thus leading to the conclusion that the same mechanisms are governing tool wear (abrasive and diffusion wear, in addition to adhesive wear). At the beginning of the test (Fig. 16a) the flank face presents signs of abrasive wear (characterized by grooves) and diffusion wear (smooth surface). The rake face shows evidence of diffusive wear due to the intimate contact between the adhered work material and the tool. At the end of life (Fig. 16b), the flank face shows accentuated abrasive wear, as can be noted by the increase in the number of grooves on the surface. Diffusion wear remains present on both flank and rake faces, as can be noticed by a smooth appearance. The rough aspect in the flank face suggests adhesive wear with the typical loss of material at granular level.

The average PSD values for the AlCrN coated tool when turning with cutting speed of 250 m/min, feed rate of 0.15 mm/rev and depth of cut of 0.25 mm (Fig. 17) show excitation of the frequency bands related to adhesive wear (from 0 to 90 kHz) and abrasive wear (300–500 kHz) at the beginning of tool life. Toward the end of life, the PSD values show the excitation of adhesive wear (0–90 kHz), the band related to the movement of dislocations and particle interactions (from 120 kHz to 280 kHz). Dislocations movement is expected to happen throughout the use of the tool and the corresponding band appears at the end of tool life only. Furthermore, the excitation of the frequency band related to abrasive wear (from 300 kHz to 480 kHz) and the frequency band of 510–600 kHz are recorded. This band is within the band excited by crack propagation (350–550 kHz) and Fig. 18c shows fracture of the wedge at the end of life as the result of cracks growth.

The AlCrN coated tool in turning at cutting speed 250 m/min, feed rate 0.15 mm/rev and cutting depth 0.25 mm, in the first pass (Fig. 18a) showed abrasive wear at the flank face. It removed the coating from the surface in the region near the interface, which certainly promotes diffusion wear due to chemical affinity between iron (in the workpiece) and cobalt (in the tool). At the rake face, abrasive wear removed the coating, after which the interaction between abrasive, adhesive and diffusive wear promoted the crater wear. In the second pass (Fig. 18b), the flank face suffered abrasive wear at the interface between the flank and the rake face and diffusion wear in the region where there was removal of the coating film. At the rake face, abrasive wear promoted the removal of coating and adhesive wear was responsible for its delamination, facilitating the action of diffusive wear which promoted the removal in depth from the surface promoting increased crater wear. In the third pass (Fig. 18c), the flank face of the tool fractured at the edge/interface with the rake face. There was also diffusive wear at the rake face, characterized by smooth surface appearance. At the rake face, the depth of the crater reached a great level, promoted by diffusive mechanism, being confused with flank wear, losing the cutting edge in a process which involved fractures.

The average PSD for the nanostructured AlCrN coated tool when turning at a cutting speed of 250 m/min, feed rate of 0.15 mm/rev and depth of cut of 0.25 mm is shown in Fig. 19.

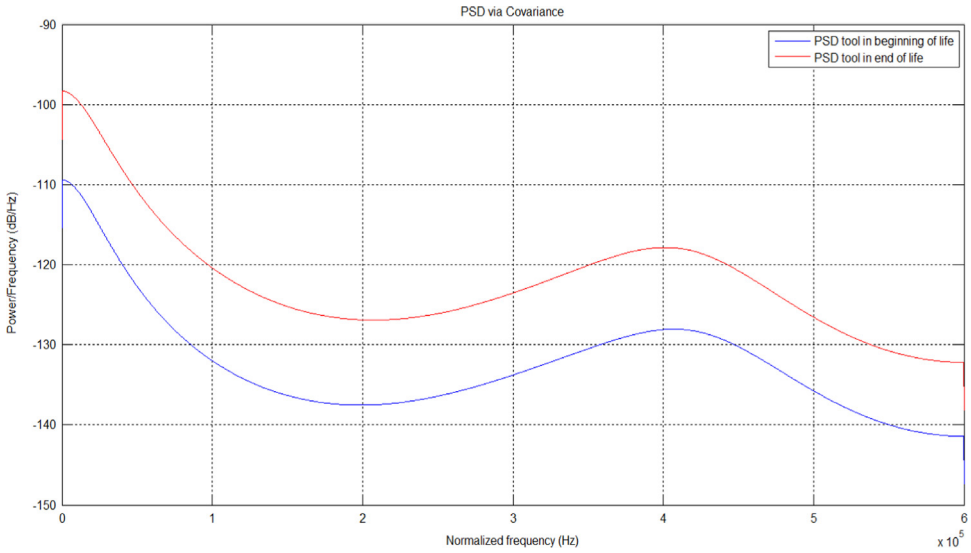

Fig. 15. PSDs of AE signals at the beginning and end of life of the uncoated tool when turning AISI 4340 steel with cutting speed of 250 m/min, feed rate of 0.15 mm/rev and depth of cut of 0.25 mm.

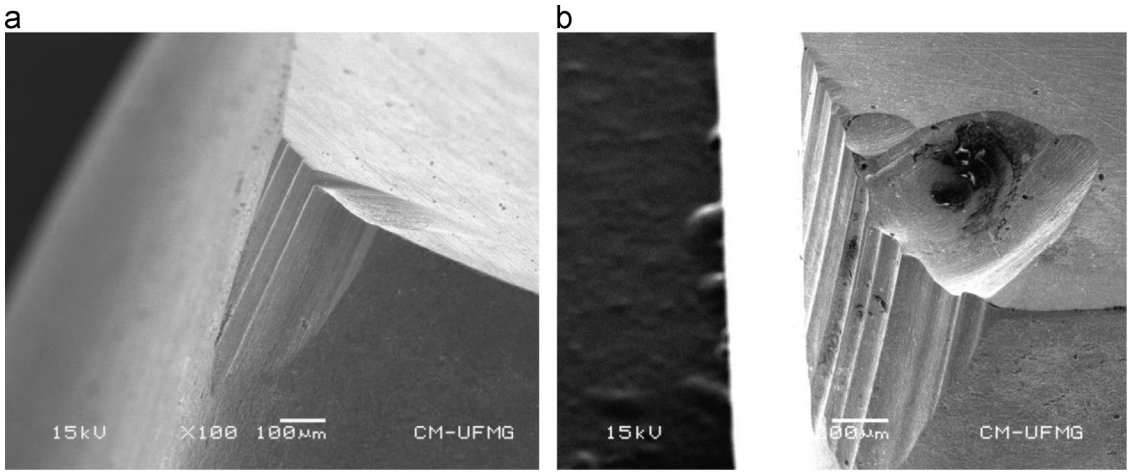

Fig. 16. SEM micrographs of a worn uncoated tool after turning with cutting speed of 250 m/min, feed rate 0.15 mm/rev and depth of cut of 0.25 mm. (a) First pass, (b) second pass.

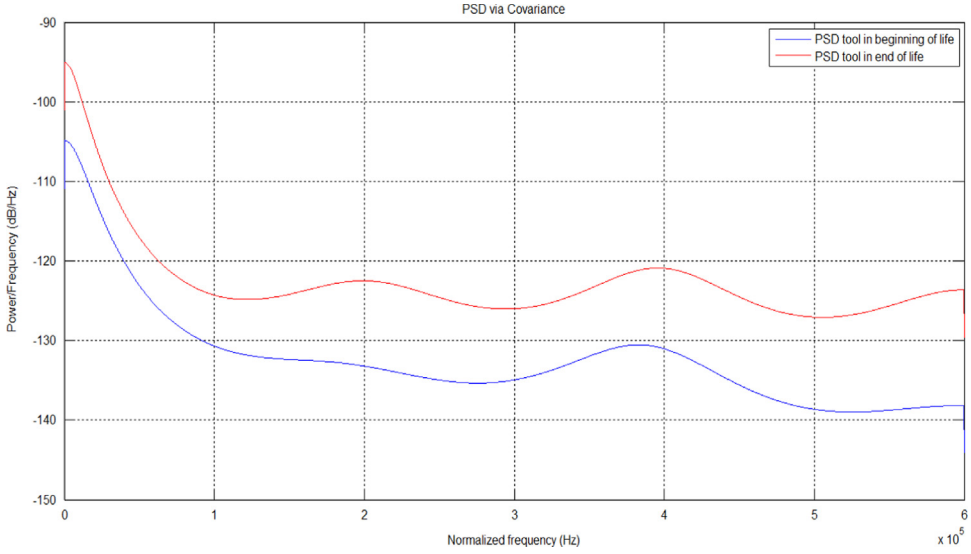

Fig. 17. PSDs of AE signals at the beginning and end of life of the AlCrN coated tool when turning AISI 4340 steel with cutting speed of 250 m/min, feed rate of 0.15 mm/rev and depth of cut of 0.25 mm.

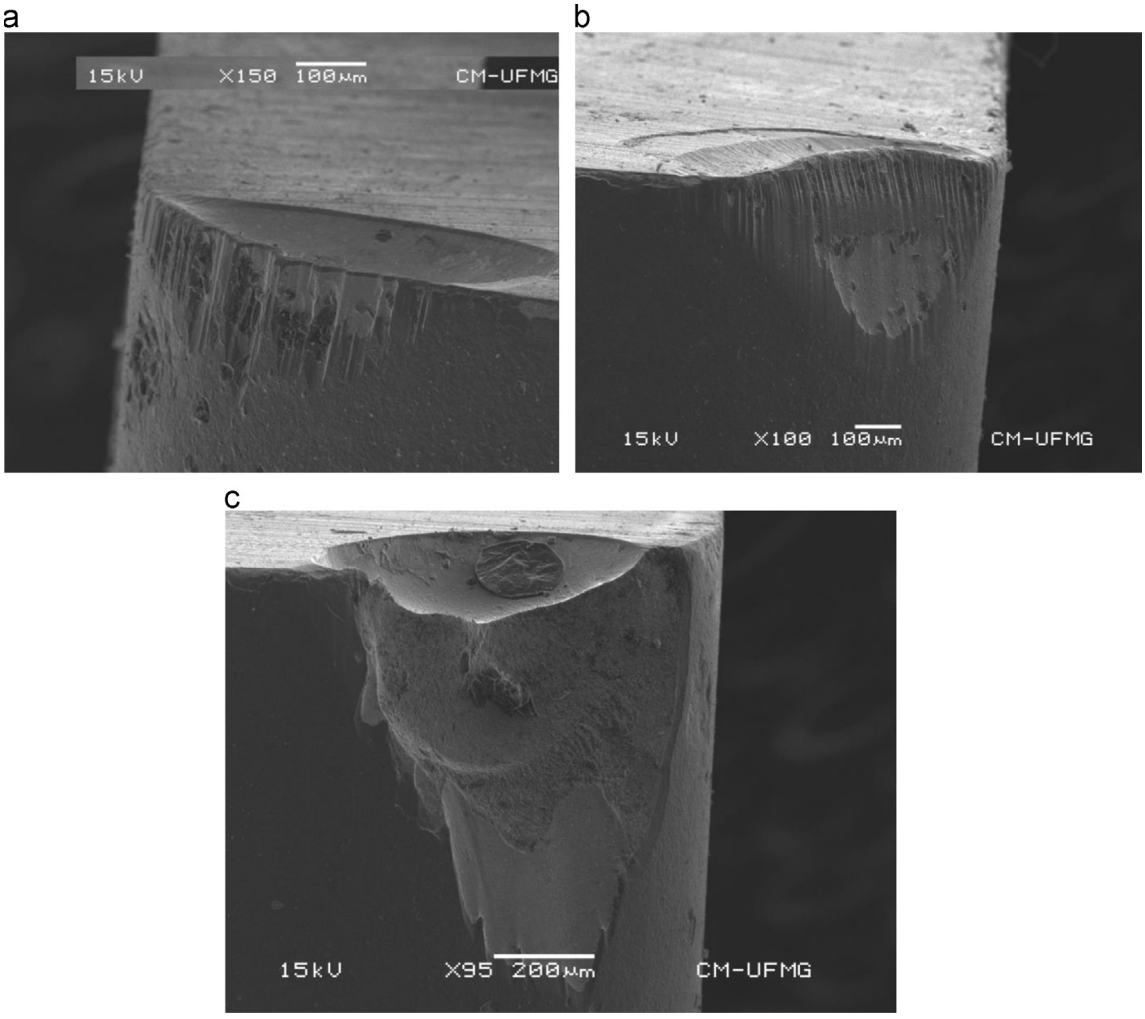

Fig. 18. SEM micrographs of AlCrN coated tool showing the wear in turning with cutting speed of 250 m/min, feed rate of 0.15 mm/rev and depth of cut of 0.25 mm. (a) First pass, (b) second pass, (c) third pass.

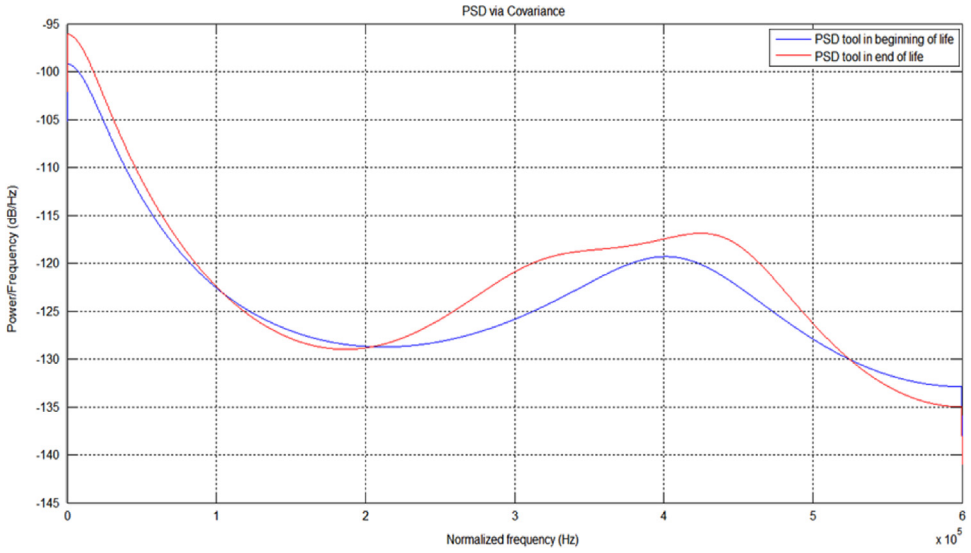

Fig. 19. PSDs of AE signals at the beginning and end of life of the nanostructured AlCrN coated tool when turning AISI 4340 steel with cutting speed of 250 m/min, feed rate 0.15 mm/rev and depth of cut of 0.25 mm.

Two frequency ranges are evident at the beginning of the test: 0–90 kHz (associated to adhesive wear) and 250–530 kHz (related to abrasive wear). Fig. 20a shows abrasive wear dominating flank wear at the beginning of tool life. The frequency band from 0 to 90 kHz is still excited at the end of life, suggesting that adhesive wear is present under this condition. Moreover, adhesive wear is

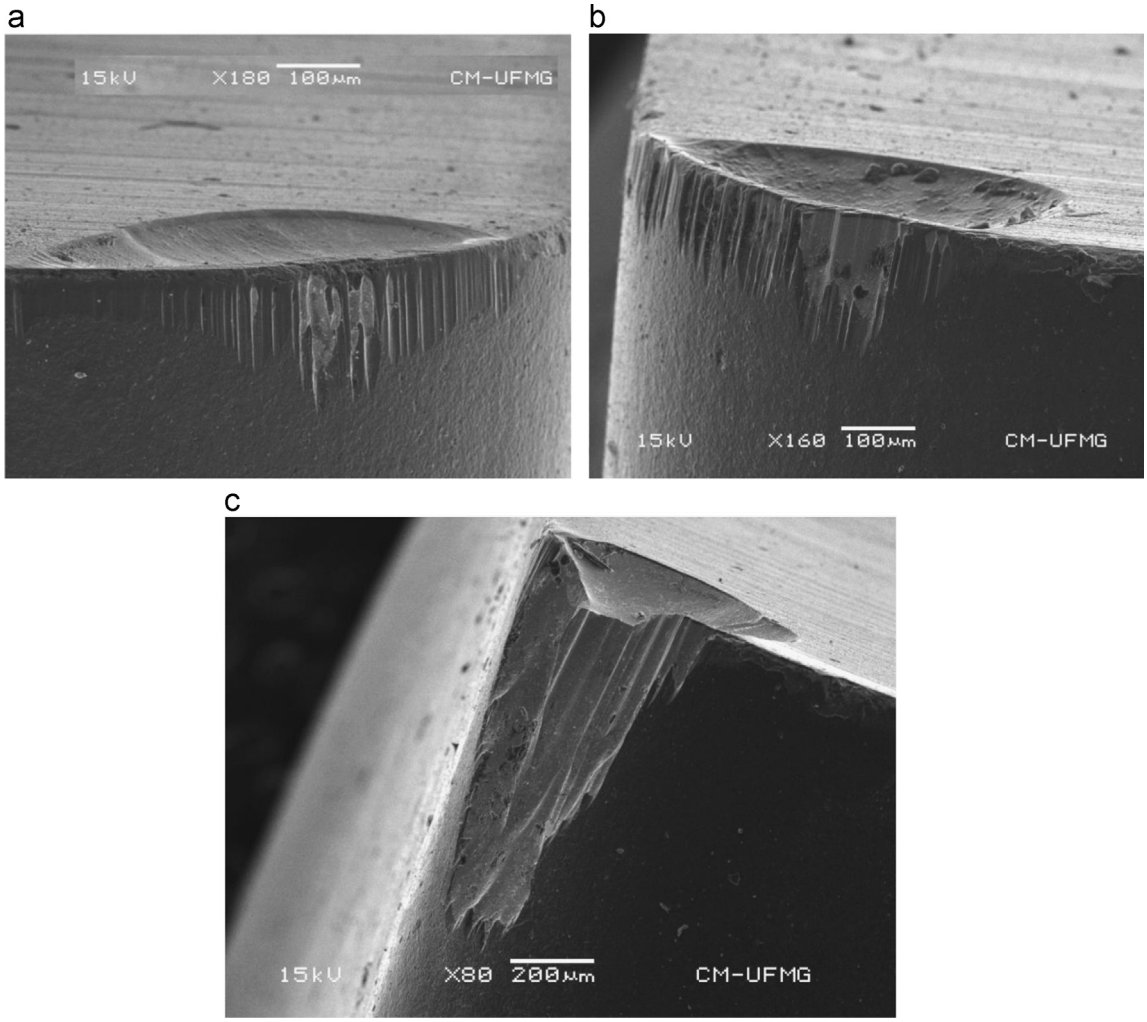

Fig. 20. SEM micrographs of a worn nanostructured AlCrN coated tool after turning with cutting speed of 250 m/min, feed rate of 0.15 mm/rev and depth of cut of 0.25 mm. (a) first pass, (b) second pass, (c) third pass.

present in all turning tests, regardless of the cutting conditions. The frequency band of 200–550 kHz is also excited and can be related to abrasive wear, which is intensively present at the end of life, as shown in Fig. 20c.

As previously discussed, after the first pass using the nanostructured AlCrN coated tool at a cutting speed of 250 m/min, feed rate of 0.15 mm/rev and cutting depth of 0.25 mm (Fig. 20a) and the flank face showed grooves typical of abrasive wear. The coating was removed at some points, thus allowing diffusive wear take place. At the rake face, the coating was removed and diffusive wear promoted the formation of a crater. After the second pass (Fig. 20b), the grooves were still present, in addition to a more severe removal of the coating in certain regions, thus increasing the diffusive wear rate. At the tool rake face, the depth of the crater increased due to diffusive and abrasive wear. After the third pass (Fig. 20c), the grooves caused by abrasion increased in the flank face and the coating was removed completely. The depth of the crater increased due to adhesive and diffusive wear. The nanostructured AlCrN coated tools presented superior performance compared with the AlCrN coated tools, as indicated by the micrographs and the flank wear evolution. Delamination of AlCrN coating was observed. In addition, the excitation of the frequency bands and the increase of amplitudes of the PSD signals can be related to the wear mechanisms observed in the micrographs and to the wear rates.

4. Conclusions

This work reports turning tests on hardened AISI 4340 steel using uncoated and coated (ordinary and nanostructured AlCrN) tungsten carbide inserts ISO grade K. Tool life and wear mechanisms were assessed and the acoustic emission signal was collected during the trials and further processed using the PSD and autocovariance techniques. Therefore, the following conclusions can be drawn:

- The presence of coating results in longer tool life without significant differences in the performances of the ordinary and nanostructured AlCrN coatings.
- Monitoring tool wear through the acoustic emission signal processed using the average PSD is sensitive to the wear rate, responding with high signal value at the beginning of tool life, followed by a decrease at the middle of life (when the wear rate is lower) and increasing at the end of tool life when the wear rate becomes higher.
- The above mentioned approach is effective for the detection of wear mechanisms, as the frequencies excited by each mechanism can be accurately determined.
- While the increase in temperature attenuates the AE signals, it does not affect the intensity of signals processed using the proposed approach.

Acknowledgments

The authors would like to thank Oerlikon Balzers (Jundiaí, Brazil) for coating the cutting tools and the ISCAR Brazil by the supply the tools.

References

[1] Bartarya G, Choudhury SK. State of the art in hard turning. Int J Mach Tools Manuf 2012;53:1–14.
[2] Meyer R, Köhler J, Denkena B. Influence of the tool corner radius on the tool wear and process forces during hard turning. Int J Adv Manuf Technol 2012;58:933–40.
[3] Sahoo AK, Sahoo B. Experimental investigations on machinability aspects in finish hard turning of AISI 4340 steel using uncoated and multilayer coated carbide inserts. Measurement 2012;45(8):2153–65.
[4] El Hakim MA, Abad MD, Abdelhameed MM, Shalaby MA, Veldhuis SC. Wear behavior of some cutting tool materials in hard turning of HSS. Tribol Int 2011;44:1174–81.
[5] Camargo JC, Dominguez DS, Ezugwu EO, Machado AR. Wear model in turning of hardened steel with PcBN tool. Int J Refract Met Hard Mater 2014;47:61–70.
[6] Lee DE, Hwang I, Valente CMO, Oliveira JFG, Dornfeld DA. Precision manufacturing process monitoring with acoustic emission. Int J Mach Tools Manuf 2006;46:176–88.
[7] Hashimoto F, Gallego I, Oliveira JFG, Barrenetxea D, Takahashi M, Sakakibara K, et al. Advances in Centerless Grinding Technology. CIRP Ann 2012;61(2):747–70.
[8] Hase A, Wada M, Koga T, Mishina H. The relationship between acoustic emission signals and cutting phenomena in turning process. Int J Adv Manuf Technol 2014;70:947–55.
[9] Li X, Brief A. Review: acoustic emission method for tool wear monitoring during turning. Int J Mach Tools Manuf 2002;42:157–65.
[10] Sikorski W. Acoustic emission. 1st ed.. Croatia: InTech; 2012.
[11] Sarychev GA, Schavelin VM. Acoustic emission method for research and control of friction pairs. Tribol Int 1991;24(1):11–6.
[12] Hase A, Mishina H, Wada M. Correlation between features of acoustic emission signals and mechanical wear mechanisms. Wear 2012;292–293:144–50.
[13] Wada M, Mizuno M, Sasada T. Study on the in-process measurement of the friction and wear with AE technique: monitoring of seizure process through AE analysis. J Jpn Soc Precis Eng 1990;56(10):1835–40.
[14] Marinescu I, Axinte DA. A critical analysis of effectiveness of acoustic emission signals to detect tool and workpiece malfunctions in milling operations. Int J Mach Tools Manuf 2008;48:1148–60.
[15] Guo YB, Ammula SC. Real-time acoustic emission monitoring for surface damage in hard machining. Int J Mach Tools Manuf 2005;45:1622–7.
[16] Mostafapour A, Davoodi S, Ghareaghaji M. Acoustic emission source location in plates using wavelet analysis and cross time frequency spectrum. Ultrasonics 2014;54(8):2055–62.
[17] Wada M, Mizuno M. Study on friction and wear utilizing acoustic emission: relation between friction and wear mode and acoustic emission signals. J Jpn Soc Precis Eng 1989;55(4):673–8.
[18] Ferrer C, Salas F, Pascual M, Orozco J. Discrete acoustic emission waves during stick–slip friction between steel samples. Tribol Int 2010;43:1–6.
[19] Chung KH, Oh JK, Moon JT, Kim DE. Particle monitoring method using acoustic emission signal for analysis of slider/disk/particle interaction. Tribol Int 2004;37:849–57.
[20] Baranov VM, Kudryavtsev E, Sarychev G, Schavelin V. Acoustic emission in friction. 1st ed.. Oxford: Elsevier; 2007.
[21] Ramadan S, Gaillet L, Tessier C, Idrissi H. Detection of stress corrosion cracking of high-strength steel used in pre stressed concrete structures by acoustic emission technique. Appl Surf Sci 2008;254:2255–61.
[22] Sasada T, Norose S. The formation and growth of wear particles through mutual material transfer. In: Proceedings of the JSLE-ASLE International Lubrication Conference of 1975 Amsterdam; 1976 p. 82–91.
[23] Williams AB, Taylor FJ. Electronic filter design handbook. 4th ed.. New York: Mcgraw-Hill; 2006.
[24] Dias MHC. Estimation of the responses of the real channel mobile radio propagation in spatial and temporal domains: noise suppression analysis by wavelet decomposition as a complementary technique for processing. In Electrical Engineering (in Portuguese). PUC-Rio; 2003 Ph.D. thesis.
[25] Bhuiyan MSH, Choudhury IA, Dahari M. Monitoring the tool wear, surface roughness and chip formation occurrences using multiple sensors in turning. J Manuf Syst 2014;33(4):476–87.
[26] Kilundua B, Dehombreuxa P, Chiementinb X. Tool wear monitoring by machine learning techniques and singular spectrum analysis. Mech Syst Signal Process 2011;25(1):400–15.
[27] Marinescu I, Axinte D. A time–frequency acoustic emission-based monitoring technique to identify workpiece surface malfunctions in milling with multiple teeth cutting simultaneously. Int J Mach Tools Manuf 2009;49(1):53–65.
[28] Hase A, Wada M, Mishina H. Correlation of abrasive wear phenomenon and AE signals. Jpn J Tribol 2006;51(10):752–9.
[29] Trent EM, Wright PK. Metal Cutting. 4th ed.. Woburn: Butterworth–Heinemann; 2000.
[30] Shaw MC. Metal Cutting Principles. 2nd ed.. New York: Oxford University Press; 2005.
[31] Holmberg K, Matthew A. Coatings tribology: properties. 2nd ed.. Amsterdam: Elsevier; 1998.
[32] Dolinsek S, Kopac J. Acoustic emission signals for tool wear identification. Wear 1999;225–229:295–303.
[33] Sviridenok AI, Kalmykova TF, Kholodilov OV. Study of real area of friction polymer-metal contact using acoustic emission. Sov J Frict Wear 1982;3(5):808–12.